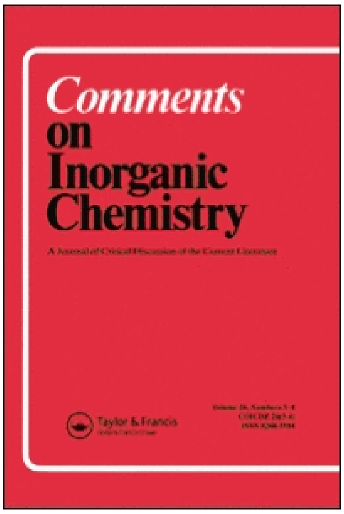

Comments on Inorganic Chemistry
Publication details, including instructions for authors and subscription information:
http://www.informaworld.com/smpp/title~content=t713455155

Aromaticity and Agostic Interactions as Stabilizing Factors in Trinuclear Rhenium Clusters with Low Electron Count

Carlo Mealli[a]; Davide M. Proserpio[a]
[a] Istituto per lo Studio della Stereochimica ed Energetica dei Composti di Coordinazione, Firenze, Italy

To cite this Article Mealli, Carlo and Proserpio, Davide M.(1989) 'Aromaticity and Agostic Interactions as Stabilizing Factors in Trinuclear Rhenium Clusters with Low Electron Count', Comments on Inorganic Chemistry, 9: 1, 37 — 59
To link to this Article: DOI: 10.1080/02603598908035802
URL: http://dx.doi.org/10.1080/02603598908035802

Aromaticity and Agostic Interactions as Stabilizing Factors in Trinuclear Rhenium Clusters with Low Electron Count

CARLO MEALLI and DAVIDE M. PROSERPIO
Istituto per lo Studio della Stereochimica ed
Energetica dei Composti di Coordinazione,
C.N.R., Via J. Nardi 39,
50132 Firenze, Italy

The uniquely featured overall Re=Re double bond structure in some classes of Re_3 clusters is critically analyzed. Perturbation MO theory, fragment frontier orbitals and other qualitative concepts based on extended Hückel calculations are applied to the well known family of clusters whose precursor is the $Re_3Cl_{12}^{-3}$ cluster. Twelve electrons from three d^4 Re(III) metals are populating σ and $\pi_\perp$ MO levels whose distribution assumes the character of either σ and $\pi_\perp$ aromaticity. In particular the $\pi_\perp$ aromaticity of six electrons distributed over three rather than six atomic centers is attributable to the availability of metal d_δ orbitals. Similarities and differences between the most classical aromatic system, i.e., benzene, are pointed out. $\pi_\perp$ aromaticity is also the most stabilizing factor in the class of alkylated clusters derived from Re_3Cl_9 [e.g., $Re_3(CH_3)_9$]. Here the metal electron deficiency [total electron count = 30] is partially overcome by *agostic interactions* between the metal atoms and the C–H bonds of the bridging CH_3 groups which then become formal four electron donors. These latter interactions are proved to be at work by closely analyzing available structural data and by calculating their stabilizing effect at EHMO level. Finally, the reported compound $Re_3(PEt_2Ph)_2(CH_3)_6(\mu\text{-}CH_3)_3$ is critically analyzed and a possible alternative formulation is forwarded.

Key Words: *trinuclear rhenium clusters, MO analysis, aromaticity in metal systems, agostic interactions*

Comments Inorg. Chem.
1989, Vol. 9, No. 1, pp. 37–59
Reprints available directly from the publisher
Photocopying permitted by license only

I. INTRODUCTION

Three-membered rings, whose atoms are mutually connected by double bonds, are uniquely featured in chemistry for a class of trinuclear rhenium clusters. The precursor is the anion $Re_3Cl_{12}^{-3}$,(**I**), (42 electrons) whose experimental X-ray structure[1] showed three equivalent Re–Re bonds as short as 2.47 Å. The bonding network (**II**) was proposed by Cotton and Haas on the basis of convincing MO arguments.[2]

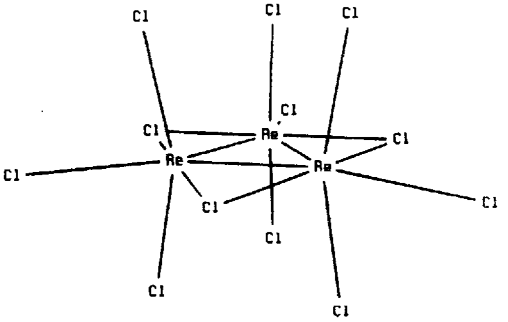

(I)

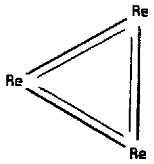

(II)

Later work has shown that some of the terminal chloride ligands can be in part substituted in (I) by other halogens or σ-donor ligands (H_2O, R_3P, etc.).[3] Also, the removal of up to three terminal ligands in the equatorial plane (L_{eq}), to yield Re_3X_9 species (36 electrons), does not have dramatic effects on the strength of the metal–metal bonds which range approximately between 2.34 and 2.48 Å. The metal atoms reach a formal eighteen electron count in $Re_3Cl_{12}^{-3}$ through the formation of three Re=Re bonds. This strongly interconnected skeleton is maintained upon departure of any L_{eq} ligand, although the corresponding metal is attributed only 16 electrons. The opposite way to look at this feature is that each metal atom in Re_3X_9 exerts residual electrophilicity in the equatorial plane. This is demonstrated by the case with which extra monodentate ligands L_{eq} are accepted by Re_3X_9 species or by the propensity of Re_3X_9 (X = Cl, I) to adopt polymeric arrangements in the solid state.[4] In any case, however, the remarkably long Re–L_{eq} bond [e.g., Re–P of 2.70 Å in $Re_3Cl_9(PEt_2Ph)_3$][5] indicates that the presence of the equatorial ligands, hence the electron saturation, is not vital for the cluster but it quenches residual metal acidity. Finally, most remarkable are the alkyl-substituted Re_3R_9 clusters[6] with a total electron count as low as 30. If the alkyl groups continue to donate a maximum of two electrons even when they are in bridging position, then the electron count of each metal is as low as 14. Still, the Re_3 bonding network (**II**) appears essentially unaffected.

Although the electronic structure of the clusters $Re_3X_{12}^{-3}$ and Re_3X_9 has already been investigated in the fine detail by other authors,[7] we devote the present Comment to underline some remarkable features, mainly illustrating the relationships between structure and bonding. Some aspects have not received the necessary attention as yet. One of these is the very high stability of the Re_3 framework which, we will show, is attributable to a double pattern of σ and π aromaticity. In addition, Re–(C–H) *agostic interactions*,[8] not previously identified, can be demonstrated to be at work in some electron-deficient alkyl derivatives. Our analysis is based on the reexamination of the experimental data reported in the literature and it is supported by qualitative MO arguments (derivable from extended Hückel calculations). Formalisms such as Fragment Orbital analysis (FMO method) and the *isolobal analogy* concept are used throughout the paper.[9] A pictorial aid is provided by the new program CACAO which, by drawing three-dimensional molecular and fragment orbitals, simplifies greatly the exposition of the numerical results.[10]

II. σ AND π AROMATICITY IN $Re_3X_9(\mu\text{-}Cl)_3^{-3}$ and $Re_3X_6(\mu\text{-}Cl)_3$ MODELS [X = MONODENTATE ANION]

EHMO calculations for the model $Re_3H_6(\mu\text{-}Cl)_3^{-3}$ reproduce essentially the level ordering previously obtained by mean of Xα, Fenske–Hall and another pioneering MO treatment.[2,7] Thus in the D_{3h} symmetry the twelve metal electrons are distributed in M–M bonding MOs, spanning the symmetries a_1', e', e'' and a_2''. The primed levels correspond to the MO equivalent of three Re–Re σ (in-plane) bonds, while the double-primed ones correspond to the three $\pi_\perp$ (out-of-plane) bonds.

We believe that the above MO set becomes more familiar if illustrated through the formalism of interacting FMOs. Initially the rhenium atoms are taken as square planarly coordinated (each chlorine bridge acts as the equivalent of two overlapping terminal ligands). No relaxation of the H_{ap}–Re–H_{ap} angles (α = 180°) is allowed after the ideal departure of the H_{eq} ligands from $Re_3H_9(\mu\text{-}Cl)_3^{-3}$. Later on, it will be shown that the total energy minimizes at a α value of ~150°.

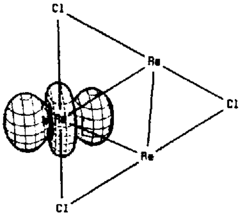

(III)

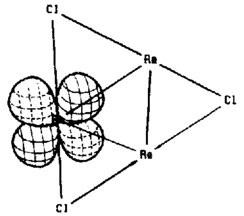

(IV)

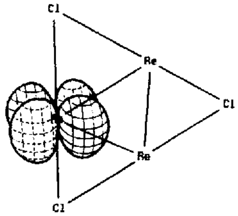

(V)

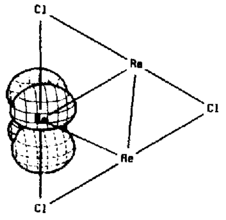

(VI)

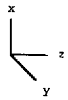

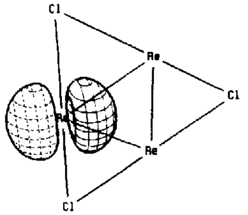

(VII)

In the model adopted each metal uses four of the nine basis orbitals (d, s and p) to form metal–ligand bonds. There remain five orbitals, **(III)**–**(VII)** which have, in the ascending energy order, the following characters: σ (radial) $[z^2]$, σ (tangential) $[xz]$, $\pi_\perp$(radial) $[yz]$, $\pi_\perp$ (tangential) $[xy]$, σ (radial) $[p_z]$. The distinction between radial and tangential character for $\pi_\perp$ orbitals is made on the basis of the directionality of their lobes above and below the Re_3 plane. Thus the orbital **(VI)**, with actual δ character, is considered tangential. Also notice that analogously to monomeric square planar d^8-L_4M complexes, the metal p_z orbitals **(VII)** lie at high energy; hence they can remain unpopulated and excluded from the important interactions.[11] However, the latter orbitals are the source of residual metal acidity. Finally, recall that each rhenium(III) d^4 ion has one electron available for each of the orbitals **(III)**–**(VI)**.

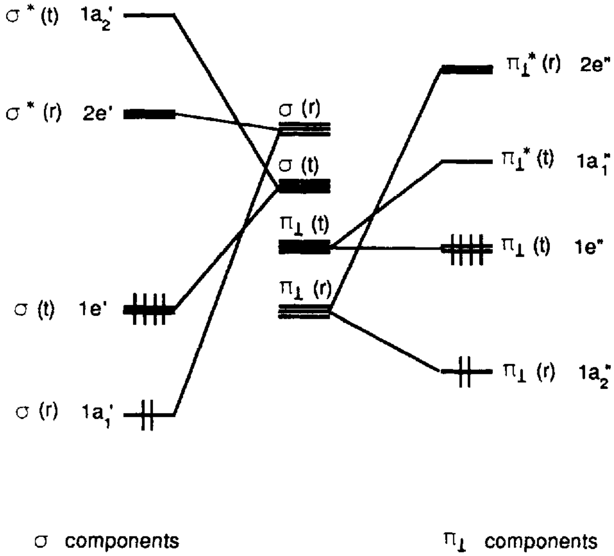

(VIII)

As shown in **(VIII)**, by separating the σ and $\pi_\perp$ components from each metal, two major MO patterns can be constructed. Both of them are characterized by three low lying occupied (M–M bonding) below three high empty (M–M antibonding) levels. The scheme corresponds to a double aromaticity either of σ or $\pi_\perp$ type.

σ aromaticity corresponds to a MO concept generally accepted to justify the strong C–C bonds in the otherwise strained molecule of cyclopropane.[12] It has also received wide support by the work of Dewar.[13] As shown in a previous paper dealing with L_6M_3 clusters (M = Ni, Pd, Pt), through the use of the *isolobal analogy* concept, σ aromaticity can be extended to inorganic triangular arrays.[14]

Here we remark on some points of interest. The so-called σ aromaticity in cyclopropane has been indicated by some authors[15] as a combination of two different types of aromaticity, namely of

Hückel and *Möbius* type. The distinction comes from the fact that the radial [as in (**III**)] and the tangential [as in (**IV**)] basis functions act separately, i.e., the radial orbitals give rise to the *Hückel* type σ aromaticity [*one filled* $(1a_1')$ *below two empty levels* $(2e')$, $4n + 2$ *rule*] while the tangential ones give rise to the *Möbius* type σ aromaticity [*two filled* $(1e')$ *below one empty level* $(1a_2')$, $4n$ *rule*].[16] Complessively, however, the pattern is that typical for six aromatic electrons in three filled below three empty levels. Since the symmetry of a triangle is at best D_{3h}, some mixing between filled (largely tangential) and empty (largely radial) e' levels is in theory allowed. The larger the mixing, the more electrons are driven into the antibonding radial $2e'$ set, the more antiaromatic (*Hückel*) becomes the system. The latter possibility is strongly limited in cyclopropane where there is a large energy gap between the two e' sets in question.

The above arguments also apply to the Re_3X_9 system where σ and $\pi_\perp$ aromaticities can be considered simultaneously active. Let us directly analyze the $\pi_\perp$ type interactions. Each metal uses the basis $\pi_\perp$ radial and tangential FMOs (**V**) and (**VI**). The final make-ups of the $\pi_\perp$ MO levels ($1a_2''$, $1e''$, $1a_1''$, $2e''$) are reported in Fig. 1. Although the two e'' sets are sufficiently separated in energy, some mixing between the radial and tangential character is apparent from the drawings [notice for example the presence in $1e''$(S) of the radial $\pi_\perp$ function from the leftmost rhenium atom]. Still we assume that the system conforms to a typical π aromatic scheme. To make the argument more convincing let us refer to benzene, the most classical among aromatic molecules. In this D_{6h} molecule, six *equal* basis p_π functions originate three bonding (a_{2u} and e_{1g}) and three antibonding (b_{1g} and e_{2u}) levels, shown at the left side of Fig. 2. We introduce now a perturbation toward D_{3h} symmetry by shrinking for example every other C=C bond of the ring. In this case the e_{1g} and e_{2u} levels descend to the same symmetry (e'') and are allowed to mix into each other. Imagine that the deformation is pursued to allow collisions of any two carbon atoms at their midpoint (hexagon → triangle). Then two consecutive in-phase p_π orbitals overlap into an unique π-radial function, whereas two out-of-phase orbitals assume the δ character implicit only in metal d orbitals. The artifact allow us to establish an ideal correlation between benzene and inorganic M_3 systems since, for spe-

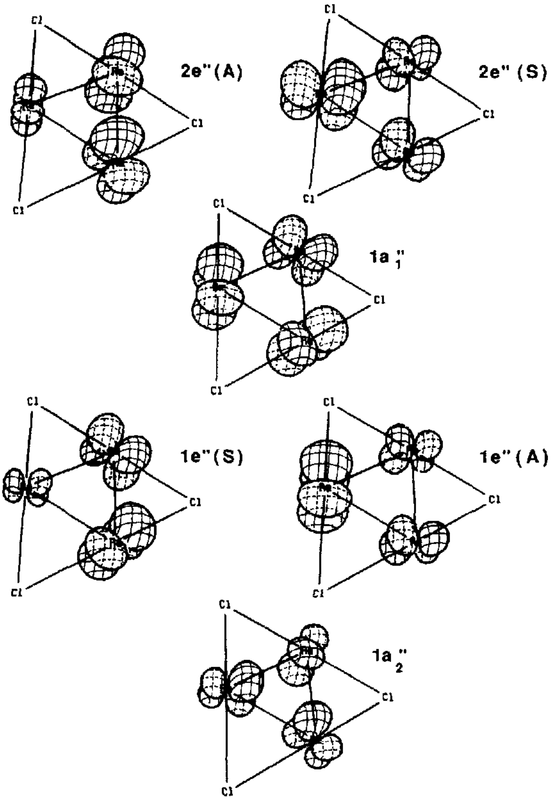

FIGURE 1 The six $\pi_\perp$ MO combinations of metal orbitals, in ascending energy order. Electron population up to the $1e''$ level mimics an aromatic-type distribution.

cial purposes, we can consider any metal center as the equivalent of two collided carbon atoms. This is envisaged on the right side of Fig. 2, where the makeup of D_{3h} benzene MOs parallels that of the $Re_3\pi_\perp$ orbitals (Fig. 1). Compare for example the $1e''$(A) levels of Re_3 and D_{3h} benzene and notice, on the left sides, the δ symmetry both at the metal atom and at the pair of carbon atoms. Analogously the in-phase combination of the p_π orbitals at the latter C_2 pair [see MO $2e''$(S)] compares with the radial $\pi_\perp$ orbital at the leftmost rhenium atom in the $2e''$(S) level of Fig. 1. Other similarities can be readily envisaged along these lines.

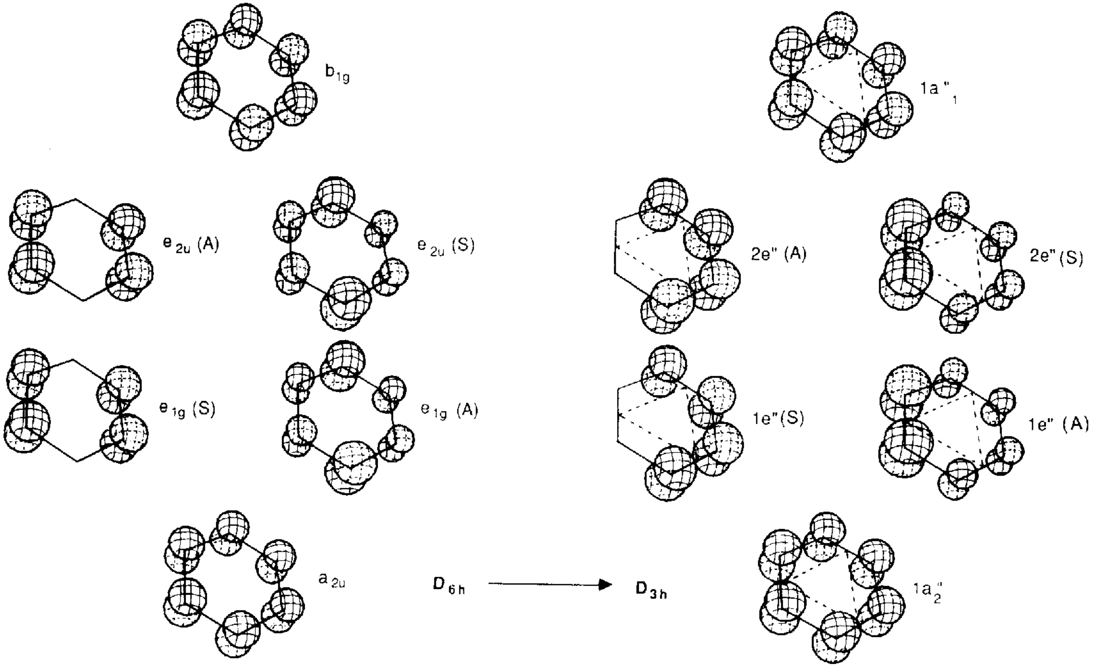

FIGURE 2 Evolution of the benzene π orbitals for shrinking every other C–C bond of the hexagon.

The above arguments support the following conclusion. Beyond the distinction between *Hückel* and *Möbius* schemes, systems able to delocalize six electrons over a *three-filled below three empty levels pattern* have the gross features of aromaticity. True six-electron aromaticity would require the existence of six *equal* basis functions, hence six atomic centers. This is the case for the somewhat ideal σ aromatic H_6 molecule or for the more realistic $\pi_\perp$ aromatic benzene. When the ring is three-membered, a *pseudo*-aromaticity can be attained by using pairs of equivalent lobes at each atomic center. As a matter of fact delocalized radial and tangential orbitals produce equivalent localized hybrids [see (**IX**)].

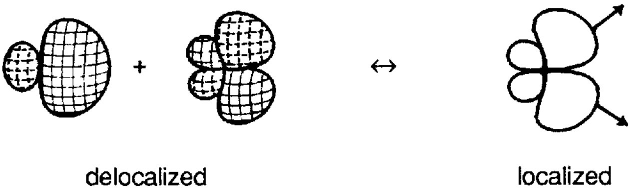

(IX)

Accordingly, three-membered rings (organic, inorganic, mixed) can all be seen to gain extra-stability from a *pseudo*-aromaticity of σ-type. By contrast $\pi_\perp$ aromaticity of six-electrons in three-membered rings can be achieved only if the atoms carry d_δ orbitals (transition elements). Besides carrying the proper electron count, the latter orbitals must be sufficiently diffuse and must have the proper energy to interact reciprocally with each other. For all of these reasons we are even more convinced that the triangular rhenium system under consideration is a unique feature in chemistry.

III. HOW THE COMPOSITION AND GEOMETRY OF THE METAL FRAGMENTS AFFECT THE STRENGTH OF THE Re–Re BONDS

As mentioned, in the model $Re_3H_6(\mu\text{-}Cl)_3$ the three H_{ap}–Re–H_{ap} angles (α) were initially fixed at 180°. By considering the bridging chlorine atoms as the equivalent of two overlapping terminal ligands (four electron donors), the coordination of each metal is square planar. If the α angle is progressively closed, each metal fragment acquires the so-called butterfly shape, frequently found in organometallic complexes (L_4M fragments with C_{2v} symmetry). The frontier orbitals of the latter are also well known.[11] Before proceeding any further we recall that the α angle is as small as $\approx$125° in some X-ray crystal structures containing Re_3L_9 units [e.g., the complex $Re_3(CH_2SiMe_3)_6(\mu\text{-}Cl_3)$, (X)].[17] Previous MO studies for the isolated Re_3Cl_9 molecule assumed an α angle of 157.8°.[7]

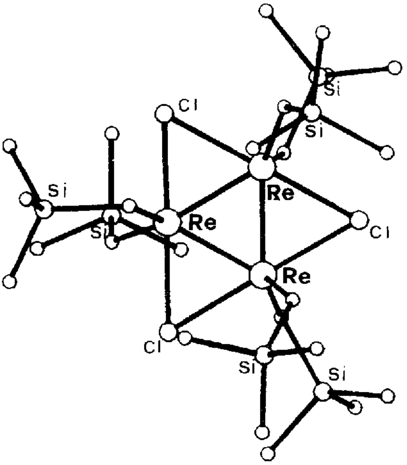

(X)

Figure 3 reports the Walsh diagram for the simultaneous closing of the three α angle from 180° to 120°. The total energy (dashed line) minimizes at $\approx$150°. The most affected levels are the $\pi_\perp(r)$ ones, i.e., the symmetry combinations of the metal orbitals yz, (V). The filled $\pi_\perp(r)$ combination ($1a_2''$ in Fig. 1) is first stabilized, but below α $\approx$160° it raises sharply in energy. By contrast the empty antibonding counterpart [degenerate $\pi_\perp^*$ (radial) $2e''$] is destabilized from the beginning. There is a ready rationale for such behavior. By pinning back the H_{ap} ligands, a σ $M-H_{ap}$ antibonding interaction is triggered which destabilizes the pure orbital d_{yz}. A rehybridization (with p_y) develops the lobes pointing inward, above and below the Re_3 plane [see **(XI)**]. Even though each single metal function is consequently raised in energy, their overall bonding

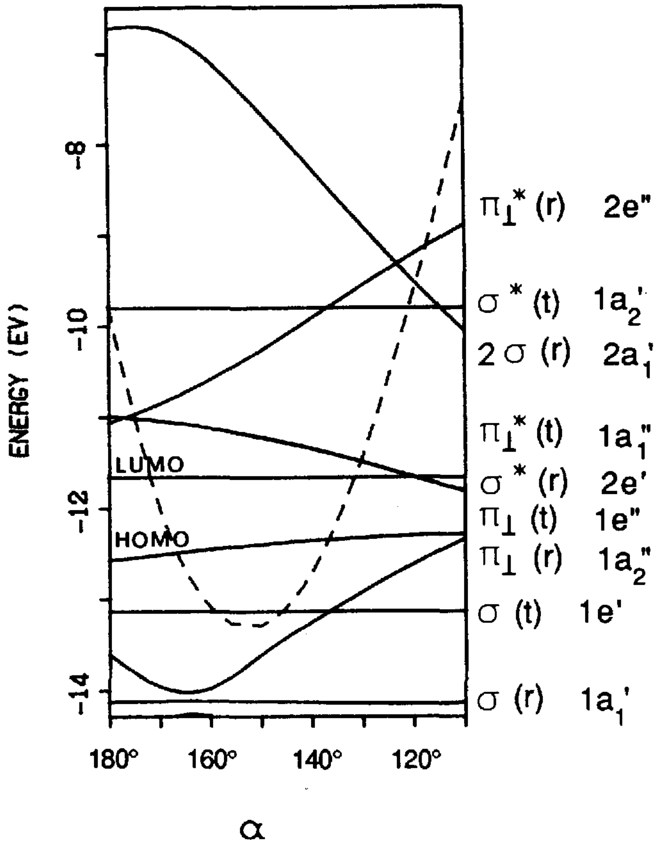

FIGURE 3 Walsh diagram and total energy variation (dashed line) parametrized by the H_{ap}–Re–H_{ap} angles (α) in the model $Re_3H_6(\mu\text{-}Cl)_3$.

combination $\pi_\perp(r)$ is initially stabilized by an increased positive overlap of the lobes in the central region. However, at a later stage ($\alpha < 160°$) the effect due to the destabilization of the single orbitals prevails. By contrast the $\pi_\perp^*(r)$ levels are immediately raised in energy due to the two combined effects [increasing metal–ligand and metal–metal antibonding]. Interestingly, we find that the Re–Re overlap population increases monotonously down to $\alpha = 120°$. Indeed, in the complex $Re_3(CH_2SiMe_3)_6(\mu\text{-}Cl_3)$, (**X**), although α is not that optimized by the EHMO calculation (125° vs. 150°), the Re–Re distance of 2.386 Å (ave.) is the shortest reported so far.

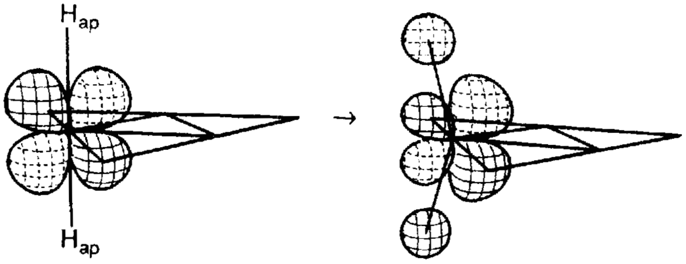

(XI)

The other effect clearly seen in the diagram of Fig. 3 is that the empty $2\sigma(r)$ $2a_1'$ combination of p_z orbitals (**VII**) is stabilized all the way. The deformation of the L_4M fragment from planarity rehybridizes the radial orbitals on each metal. In particular p_z develops in the outward direction; hence the metal acidity is enhanced, (**XII**).

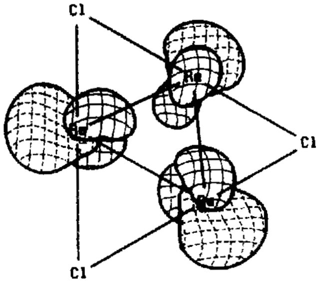

(XII)

Noteworthy is that the presence of the bulky trimethylsilymethyl groups can prevent the approach of nucleophiles to the metals and helps to stabilize the structure type (**X**). Theoretically we examine the simultaneous attack of three terminal hydride ligands to the Re_3 framework.

The correlation diagram of Fig. 4 shows that all of the combinations of the in-plane radial orbitals are affected. In particular

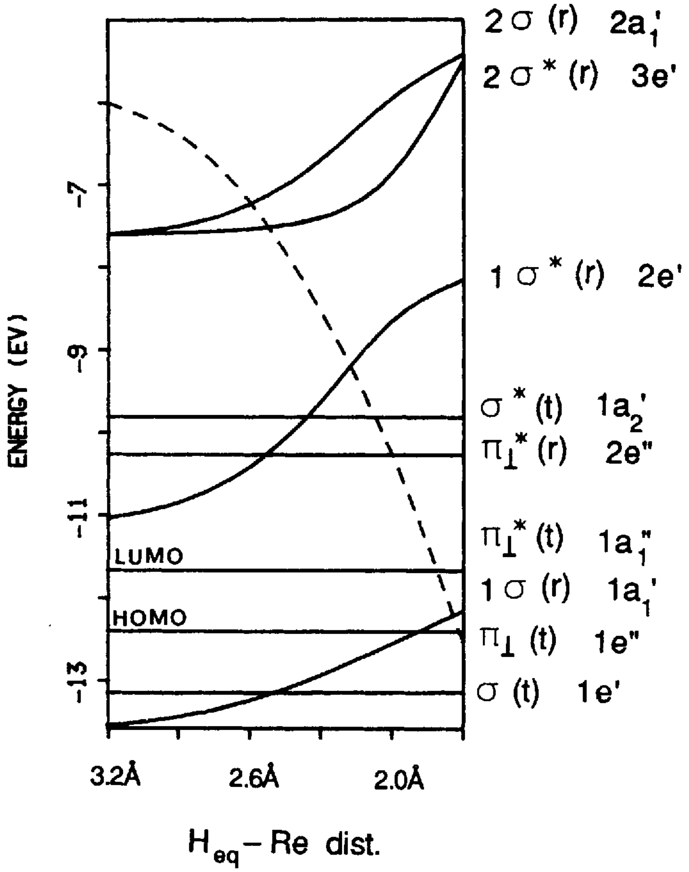

FIGURE 4 Walsh diagram and total energy variation (dashed line) as a function of the H_{eq}–Re distances (Å) in the model $Re_3H_6(H_{eq})_3(\mu\text{-}Cl)_3$.

we notice a destabilization of the in-phase $1\sigma(r)$ $1a_1'$ and $2\sigma(r)$ $2a_1'$ (**XII**) MOs as well as of the Re_3 M–M antibonding $1\sigma(r)^*$ $2e'$ set. The MO $2\sigma(r)^*$ $3e'$, which also destabilizes, has prevailing M–L antibonding character. While the destabilization of the empty levels mirrors the formation of the new Re–H_{eq} bonds, the whole system is negatively affected by the rise of the filled $1\sigma(r)$ $1a_1'$ level, which for short Re–H_{eq} distances approaches the LUMO's energy. Possibly, to avoid such a destabilizing effect, the three in-plane terminal ligands never make strong bonds to the metals in

Re_3L_{12} systems [e.g., Re–P = 2.70 Å in $Re_3Cl_6(PEt_2Ph)_3(\mu\text{-}Cl)_3$[5] and Re–$Cl_{eq}$ of 2.52 Å (vs. a Re–Cl_{ap} bond of 2.36 Å) in $Re_3Cl_{12}^{-3}$,[1]]. Another possibility exploited by the Re_3X_9 system to quench in part the metal's electrophilicity is that of accepting only one or two L_{eq} ligands. Examples are found in $Re_3ClH(PPh_3)(CH_2SiMe_3)_4(\mu\text{-}Cl)_3$[18] where only one metal atom is coordinated by as many as three terminal ligands (H, Cl, PPh_3) and in $Re_3(CH_2SiMe_3)_5[ON(CH_2SiMe_3)NO](\mu\text{-}Cl)_3$[6c] with one carbon and two oxygen donor atoms terminally linked to one metal. Two L_5Re and one L_4Re fragments are found in $Re_3X_{11}^{-2}$ species (X = Cl, Br),[19] where the Re–Re bond, *trans* to the fragment L_4Re, is longer than the other two. In the bromine cluster[19b] the resulting isosceles Re_3 triangle has a base of 2.49 Å and two sides 2.43 Å.

In general, the trends for the calculated Re–Re overlap populations are in good agreement with the experimental bond lengths. As seen the hybridization of the metal π_{-} orbitals enhances the strength of the Re–Re π bonds in Re_3X_9 clusters which contain butterfly fragments. For example, the Re–Re overlap population in the model (**X**) increases from 0.48 to 0.52 when closing α from 180° to 120°. σ effects are also operative. In fact square pyramid L_5M fragments in $Re_3X_{12}^{-3}$ compounds are expected to have a σ lobe more hybridized than the corresponding L_4M fragment, where the L_{eq} ligand is missing.[11] Accordingly, the Re–Re overlap population increases along the pathway of Fig. 4 and it is as large as 0.58 when the Re–H_{eq} bond becomes as short as 1.7 Å. However, the shorter the Re–H_{eq} bonds, the more destabilized is the system so, for longer and more realistic distances, the Re–Re overlap populations come nearer to 0.50, the value calculated for the Re_3X_9 species. Finally, in the model $Re_3H_8(\mu\text{-}Cl)_3^{-2}$ with only two in-plane terminal ligands (H_{eq}), the experimental trend[19b] toward a Re_3 isosceles triangle is reproduced [one long side (o.p. = 0.48) vs. two short ones (o.p. = 0.51)]. No bias is introduced in the calculation as the triangle is taken as equilateral. We do not present in detail the orbital effects due to the demolition of the threefold symmetry, but as already pointed out by Bursten *et al.*.[7a] the out-of-phase combination of the two incoming L_{eq} ligands interacts selectively with the antisymmetric components of the $1\sigma(r)^*$ and $2\sigma(r)^*$ levels which are Re–Re antibonding on a unique side of the triangle.

IV. AGOSTIC INTERACTIONS IN CLUSTERS CONTAINING BRIDGING ALKYL GROUPS

Reactions of the compounds of the type Re_3X_9 with a variety of Grignard reagents yield new clusters in which alkyl groups replace totally or in part the chloride ligands.[6] Some of the products which maintain the bridging chloride ligands [e.g., **(X)**] have been examined above. Most interesting appear the clusters in which the alkyl groups themselves act as bridges between rhenium atoms. In principle the latter groups are not able to act as four electron donors toward the metals and this addresses the question of the relative stability of these electron deficient clusters. An immediate answer provided by our MO analysis is that the distribution of the twelve metal electrons remains substantially similar to that of scheme **(VIII)**. Accordingly the σ or $\pi_\perp$ aromaticities can account by themselves for the stabilization of these unusual low-electron count clusters. Moreover, a detailed analysis shows other remarkable features. As reference compound we use the cluster $Re_3Cl_3(CH_2SiMe_3)_3(\mu\text{-}CH_2SiMe_3)_3$[18] with 30 valence electrons. Although not located in the published structure, the hydrogen atoms at the bridging CH_2SiMe_3 groups are shown in the drawing **(XIII)**, based on the coordinates of the Cambridge Structural Database (CSD).[20]

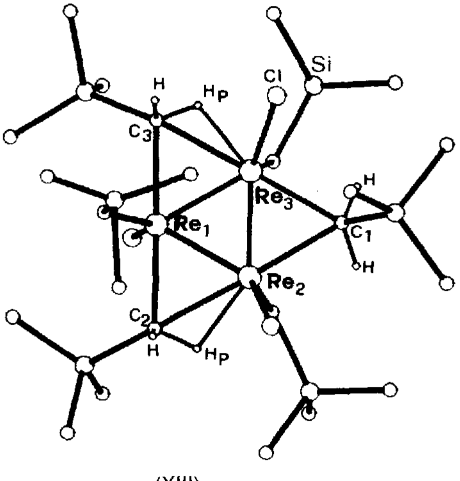

(XIII)

Given the presence of a bulky $SiMe_3$ substituent at each bridging carbon atom, it has been possible to calculate the hydrogen positions on the assumption that carbon atoms remain roughly tetrahedral. For example, two equal Re–C–Si angles ($\approx 127°$) at the C_1 bridge indicate that the ideal threefold axis of the substituted methyl group is directed toward the center of the Re_3 triangle. By contrast the two Re–C–Si angles at the other two C bridges measure $\approx$ 111° and 156°, respectively. Accordingly, the directions of the alkyl pseudo-threefold axes coincide almost with the two Re_1–C_3 and Re_1–C_2 bonds. It is clear from (**XIII**) that the two H_p atoms are practically constrained in the Re_3 plane and are involved in *agostic* [Re–(C–H)] *interactions*.[8] Such a new awareness allows us to investigate how the *agostic interactions* provide extra electronic stability to the system.

Our starting model has three equivalent bridging methyl fragments oriented as the unique CH_2SiMe_3 group in (**XIII**), i.e., the main CH_3 axes are all directed toward the center of the Re_3 triangle and no H atom lies in that plane. Since no major perturbation is introduced by rotation of CH_3 about the latter axes we have conveniently located one H atom from each CH_3 in the Re_3 plane, (**XIVb**). Then we rotate (by β angles) the CH_3 groups about axes perpendicular to the Re_3 plane and passing through the C_{bridge} atoms.

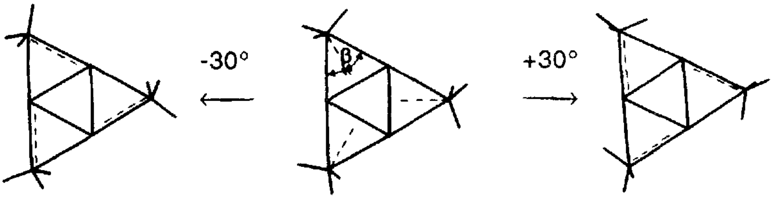

(XIVa) (XIVb) (XIVc)

As shown, ±30° β rotations bring the CH_3 axes (dashed line) collinear with the Re–Re bonds. Positive β's (**XIVc**) correspond to the largest *agostic interactions* (with three short Re–H_p distances of ~1.9 Å). Negative β's (**XIVa**) elongate Re–H_p distances but bring the out-of-plane H atoms closer to the metals (six Re–H distances being ~2.3 Å). There is an energy difference as large as

1.5 eV (ca. 35 kcal/mol) among the two limiting geometries, (**XIVc**) being the most stable. The energy of (**XIVb**) is approximately intermediate.

Importantly, the rotations of the CH_3 groups affects five metal levels reconducible to those defined in (**VIII**) and in Fig. 1: the filled doubly degenerate $\pi_{\perp}(t)$ $1e''$ stabilizes all the way, whereas three empty levels [$\sigma^*(t)$ M–M antibonding and doubly degenerate $\sigma^*(r)$ M–L antibonding] are destabilized in the β range 0°/+30°, (**XIVb → XIVc**).

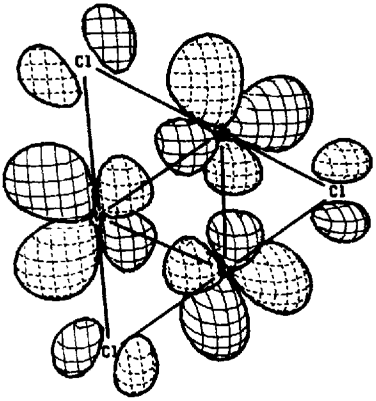

(XV)

In order to understand well the latter σ effects, we recall that in bridged chloride clusters there are combinations of filled tangential chlorine orbitals (the equivalent of the second lone pair at each chlorine) able to donate electrons to metal symmetry adapted combinations. As an example (**XV**) [$1a_2'$ in (**VIII**)] shows the antibonding interaction occurring between two $\sigma^*(t)$ sets of metal and chlorine atoms. The bridging methyl groups have no pure tangential p orbitals but still can give rise to an interaction similar to (**XV**); hence they become formal four electron donors. The populated FMO (**XVI**), having a well defined C–H bonding character, is used for the purpose. Notice that the function (hence the electron density) is not symmetrically distributed about the node through the carbon atom. Such an asymmetry is the driving force to rotate the CH_3 group and to improve the Re–(C–H) *agostic interactions*.

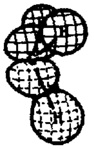

(XVI)

The drawing in (**XVII**) shows the $\sigma^*(t)$ MO [equivalent to $1a_2'$ in (**VIII**)] at its largest Re–(C–H) antibonding interaction ($\beta = +30°$). Notice that the CH_3 orbital contribution in (**XVII**) is largely that in (**XVI**) with less resolution. For analogous reasons (not shown pictorially) the degenerate $\sigma^*(r)$ set goes up in energy, while its bonding counterpart (distributed over different levels at low energy) brings stabilization to the system.

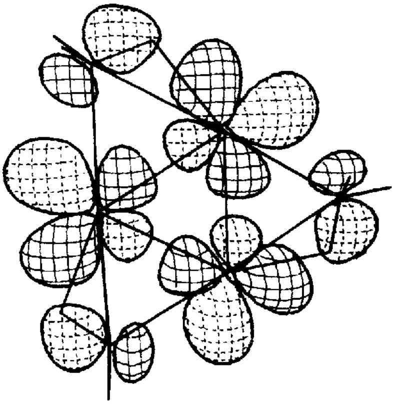

(XVII)

In going toward the form (**XIVc**), extra stabilization (but not extra metal-bridge bonding) is brought in by the descent of the $\pi_\perp(t)$ level. The degenerate $\pi_\perp(t)$ $1e''$ combination of metal orbitals in Re_3Cl_9, considered mainly Re–Re π_- bonding in Fig. 1, is indeed destabilized by an antibonding interaction with $\pi_\perp$ orbitals of chlorine (not shown in that figure). In the model with bridging methyl groups, the CH_3 $\pi_\perp$ FMO [degenerate with the in-plane C–H bonding FMO (**XVI**)] destabilizes the Re_3 $\pi_{\perp}(t)$ bonding set. As shown in (**XVIII**) for one member of the degenerate set, the shorter the metal to hydrogen (out-of-plane) distances (β = negative), the larger the destabilization. By contrast, the system is stabilized in going toward an increasing *agostic interaction* (β = positive).

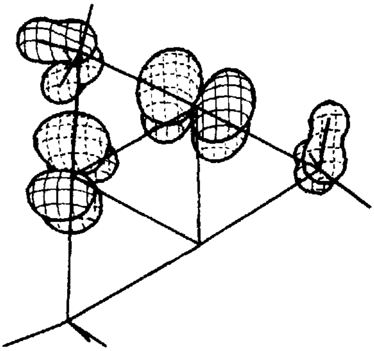

(XVIII)

In the preceeding discussion we have assumed that three *agostic interactions* are simultaneously at work, whereas the structure (**XIII**) provides evidence for only two of them. A calculation suggests that the third *agostic interaction* is responsible for an extra stabilization of ca. 0.2 eV; however, the steric hindrance of the bulky $SiMe_3$ substituents can easily account for the observed experimental geometry. Indeed three simultaneous *agostic interactions* would force the bulky substituents of terminal and bridging $CH_2(SiMe_3)$ groups to stay too close to each other.

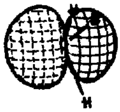

(XIX)

Finally, the reorientation of two carbon σ hybrids (**XIX**) away from the center of the Re_3 triangle toward rhenium atoms favors an asymmetry between the two Re–C bonds at each bridge, as indicated by the corresponding overlap population values. These magnitudes are large and suggest a sizeable effect on the Re$-C_{bridge}$ distances which is not experimentally confirmed. In fact the structure of the compound $Re_3Cl_3(CH_2SiMe_3)_3(\mu\text{-}CH_2SiMe_3)_3$ indicates a difference of only a few hundreds of an Ångstrom between the two C–Re bonds departing from the same bridging carbon atom. The difference is, however, in the predicted direction. By contrast a remarkable difference (2.2 vs. 2.4 Å) is found between two CH_3 bridges in the structure of $Re_3(CH_3)_6(PEt_2Ph)_2(\mu\text{-}CH_3)_3$.[6c]

V. CONSIDERATIONS ON THE COMPOUND $Re_3(CH_3)_6(PEt_2Ph)_2(\mu\text{-}CH_3)_3$

The electrophilicity inherent to the Re_3X_9 species is even more appropriate to electron deficient alkyl derivatives such as $Re_3(CH_3)_9$. Accordingly, the latter compound reacts readily with phosphine donors to give adducts such as $Re_3(PEt_2Ph)_3(CH_3)_6(\mu\text{-}CH_3)_3$.[6c] A serendipitous recrystallization of the latter yielded what has been determined as $Re_3(PEt_2Ph)_2(CH_3)_6(\mu\text{-}CH_3)_3$ on the basis of an X-ray structural analysis.[6c] No other physical–chemical characterization is reported in the original paper.

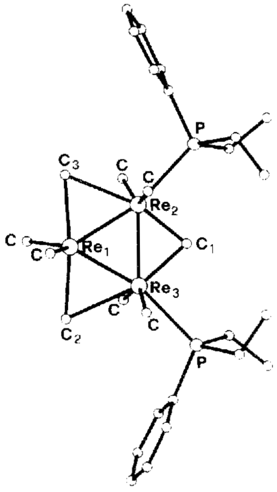

(XX)

A molecular drawing carried out by using the CSD coordinates[21] is presented in (**XX**). As already mentioned at the end of the previous paragraph, two CH_3 groups (atoms C_2 and C_3) bridge asymmetrically two Re–Re bonds. Quite surprisingly, the third CH_3 bridge makes two equal Re–C bonds as short as 1.93 Å, a distance which suggests two strong covalent interactions. The dramatic consequence of this fact is that the involved carbon atom appears as a *five-valent* one. Also by focusing on other structural details, we notice that the terminal donor atoms at either the Re_2 or the Re_3 metals are not all coplanar. In particular the four carbon atoms lie coplanar with the Re_2–Re_3 bond, while the two phosphine ligands point in radial directions. On account of such an arrangement, the phosphines together with their substituents were said to compress the central bridging methyl group.[6c] Also, it is not easy to recognize canonical fragmental geometry at the two Re_2 and Re_3 atoms. One possibility which simplifies the FMO analysis is that C_2 and C_3 atoms are not involved in bridge-bonding but form the butterfly L_4M fragment about the Re_1 atom. Consequently, the fragments at the Re_2 and Re_3 atoms appear as trigonal pyramids with an apical phosphine ligand and three equatorial carbon atoms (C_1 shares the common vertex of the two triangles). Simple reasoning based on the isolobal analogy concept supports such an interpretation; however, the stability of the molecule remains obscure. The EHMO method indicates that no appreciable HOMO–LUMO gap exists for the model $Re_3H_6(PH_3)_2(\mu\text{-}CH_3)_3$ closest to the experimental geometry of (**XX**). By approching a CH_3 group to the Re_2–Re_3 bond, one notices that one MO level is particularly destabilized. This MO identifies with the $1e''(S)$ member of the degenerate $\pi_\perp(t)$ bonding set, shown in Fig. 1. Its antibonding interaction with the FMO of CH_3 shown in (**XVI**) pushes the orbital energy to that of the LUMO [see (**XXI**)].

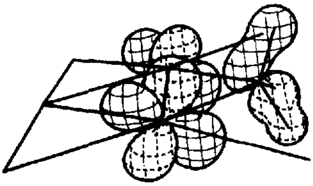

(XXI)

We could not obtain any more favorable HOMO–LUMO gap by readjusting the model's geometry, worst of all by forcing *agostic interactions*. Thus we put forward the hypothesis that the group bridging the Re_1–Re_2 bond has a nature other than methylic. A bridging methylene group can be discarded as not only do we still calculate no significant HOMO–LUMO gap, but also this would alter the charge of the cluster itself. In order to keep the cluster uncharged, the bridging group must carry monoanionic character. Among other hypotheses, a hydroxo group is a reasonable candidate. It is not in contrast with the reported structural results; in fact under X-ray least squares refinement the behavior of an oxygen atom can be similar to that of a carbon atom. Moreover, the Re–O distance in compounds containing bridged Re–O–Re moieties [1.92–1.97Å][22] coincides with that observed for the present structure. Finally the $\pi_{\perp}(t)$ bonding MO [analogous to that in (**XXI**)] is much less destabilized for the approaching of an OH group in place of CH_3 [for electronegativity reasons the $p\pi$ oxygen orbital involved does not greatly interact with the Re_3 $\pi_{\perp}(t)$ bonding MO]. Ultimately, the calculated HOMO–LUMO gap (ca. 0.6 eV) appears sufficiently large for the molecule.

We do not pretend to be conclusive on the nature of the cluster in question. New experimental evidence is certainly needed and we hope that the present Comment can promote new interest in the problem.

APPENDIX

Computational Details. All of the MO calculations were of the extended Hückel type using a modified version of the Wolfsberg–Helmholz formula. The atomic parameters for rhenium are: 6s H_{ii} $-$ 9.36 eV, ζ 2.4; 6p H_{ii} $-$ 5.96 eV, ζ 2.37; 6d H_{ii} $-$ 12.66 eV, ζ_1 5.34 (0.63555), ζ_2 2.28 (0.56738). In the model the Re–H and Re–Cl distances are 1.7 Å and 2.4 Å, respectively. Unless specified otherwise, all of the Re–Re bonds are fixed at the value of 2.40 Å.

Acknowledgment

This work has been supported in part by C.N.R. funds of the Progetto Strategico, Metodologie Cristallografiche Avanzate.

References

1. J. A. Bertrand, F. A. Cotton and W. A. Dollase, J. Am. Chem. Soc. **85**, 1349–1350 (1963).
2. F. A. Cotton and T. E. Haas, Inorg. Chem. **3**, 10–17 (1964).
3. For reviews see: (a) F. A. Cotton and R. A. Walton, *Multiple Bonds Between Metal Atoms* (Wiley, New York, 1982), Chap. 6, pp. 265–282. (b) F. A. Cotton and G. Wilkinson, *Advanced Inorganic Chemistry, Fifth Edition* (Wiley, New York, 1988), Chap. 19, pp. 852–855. (c) B. F. G. Johnson, in *Transition Metal Clusters*, ed. B. F. G. Johnson (Wiley, Chichester, 1980), Chap. 1, pp. 18–25.
4. (a) F. A. Cotton and J. T. Mague, Inorg. Chem. **3**, 1402 (1964). (b) M. J. Bennett, F. A. Cotton and B. M. Foxman, Inorg. Chem. **7**, 1563 (1968).
5. F. A. Cotton and J. T. Mague, Inorg. Chem. **3**, 1094–1098 (1964).
6. (a) K. Mertis, A. F. Masters and G. Wilkinson, J. Chem. Soc. Chem. Commun. 858–859 (1976). (b) A. F. Masters, K. Mertis, J. F. Gibson and G. Wilkinson, Nouv. J. Chim. **1**, 389 (1977). (c) P. Edwards, K. Mertis, G. Wilkinson, M. B. Hursthouse and K. M. A. Malik, J. Chem. Soc. Dalton Trans. 334–344 (1980).
7. (a) E. Bursten, F. A. Cotton, J. C. Green, E. A. Seddon and G. G. Stanley, J. Am. Chem. Soc. **102**, 955–968 (1980). (b) W. C. Trogler, D. E. Ellis and J. Berkovitz, J. Am. Chem. Soc. **101**, 5896–5901 (1979).
8. M. Brookhart and M. L. H. Green, J. Organomet. Chem. **250**, 395–408 (1983).
9. (a) R. Hoffmann and W. N. Lipscomb, J. Chem. Phys. **36**, 2179–2189 and 3489–3493 (1962); **37**, 2872 (1962). R. Hoffmann, J. Chem. Phys. **39**, 1397–1412 (1963). (b) H. Fujimoto and R. Hoffmann, J. Phys. Chem. **78**, 1167 (1974). R. Hoffmann, H. Fujimoto, J. R. Swenson and C.-C. Wan, J. Am. Chem. Soc. **95**, 7644–7650 (1973). (c) R. Hoffmann, Angew. Chem. Int. Ed. Engl. **21**, 711–724 (1982).
10. C. Mealli and D. M. Proserpio, submitted for publication.
11. T. A. Albright, J. K. Burdett and M. H. Whangbo, *Orbital Interactions in Chemistry* (Wiley, New York, 1985), Chap. 16.
12. (a) W. L. Jorgensen and L. Salem, *The Organic Chemist's Book of Orbitals* (Academic Press, New York, 1973), pp. 19–23. (b) R. Hoffmann, *Special Lectures at the 23rd International Congress of Pure and Applied Chemistry* (Butterworths, London, 1971), Vol. 1, p. 157.
13. M. J. S. Dewar, J. Am. Chem. Soc. **106**, 669–682 (1984).
14. C. Mealli, J. Am. Chem. Soc. **107**, 2245–2253 (1985).
15. K. Yates, *Hückel Molecular Orbital Theory* (Academic Press, New York, 1978), Chap. 8, pp. 297–299.
16. H. E. Zimmerman, Acc. Chem. Res. **4**, 272 (1971).
17. M. B. Hursthouse and K. M. A. Malik, J. Chem. Soc. Dalton Trans. 1334–1337 (1978).
18. K. Mertis, P. G. Edwards, G. Wilkinson, K. M. A. Malik and M. B. Hursthouse, J. Chem. Soc. Dalton Trans. 705–716 (1981).
19. (a) B. R. Penfold and W. T. Robinson, Inorg. Chem. **5**, 1758 (1966). (b) M. Elder and B. R. Penfold, Inorg. Chem. **5**, 1763 (1966).
20. Cambridge Crystallographic Data Centre, University Chemical Laboratory, Lensfield Road, Cambridge CB2 1EW, U.K., Copyright 1988.
21. The CSD reports some errors for the coordinates.
22. (a) W. A. Herrmann, R. Serrano, U. Küsthardt, M. L. Ziegler, E. Guggolz and T. Zahn, Angew. Chem. Int. Ed. Engl. **23**, 515–517 (1984). (b) W. A. Herrmann, R. Serrano, M. L. Ziegler, H. Pfisterer and B. Nuber, *ibid.* **24**, 50–52 (1985).